Advances in Nano Research, *Vol. 12, No. 2 (2022) 197-212*
https://doi.org/10.12989/anr.2022.12.2.197

Computerized bone age estimation system based on China-05 standard

Chuangao Yin*[1], Miao Zhang[2], Chang Wang[1], Huihui Lin[1], Gengwu Li[1], Lichun Zhu[1], Weimin Fei[1] and Xiaoyu Wang[3]

[1]*Anhui Provincial Children's Hospital, Hefei 230054, China*
[2]*Shijiazhuang Kid Grow Science and Technology Co. Ltd, Shijiazhuang 050000, China*
[3]*Anhui Medical University, Hefei 230032, China*

(*Received September 3, 2021, Revised December 17, 2021, Accepted December 22, 2021*)

Abstract. The purpose of this study is to develop an automatic software system for bone age evaluation and to evaluate its accuracy in testing and feasibility in clinical practice. 20394 left-hand radiographs of healthy children (2-18 years old) were collected from China Skeletal Development Survey data of 1998 and China Skeletal Development Survey data of 2005. Three experienced radiologists and China-05 standard maker jointly evaluate the stages of bone development and the reference bone age was determined by consensus. 1020 from 20394 radiographs were picked randomly as test set and the remaining 19374 radiographs as training set and validation set. Accuracy of the automatic software system for bone age assessment is evaluated in test set and two clinical test sets. Compared with the reference standard, the automatic software system based on RUS-CHN for bone age assessment has a 0.04 years old mean difference, ±0.40 years old in 95% confidence interval by single reading, a 85.6% percentage agreement of ratings, a 93.7% bone age accuracy rate, 0.17 years old of MAD, 0.29 years old of RMS; Compared with the reference standard, the automatic software system based on TW3-C RUS has a 0.04 years old mean difference, a ±0.38 years old in 95% confidence interval by single reading, a 90.9% percentage agreement of ratings, a 93.2% bone age accuracy rate, a 0.16 years of MAD, and a 0.28 years of RMS. Automatic software system, AI-China-05 showed reliably accuracy in bone age estimation and steady determination in different clinical test sets.
Keywords: AI-China-05; bone age; deep learning; RUS-CHN; TW3-C RUS

1. Introduction

An artificial intelligence bone age evaluation system for Chinese children was established based on China-05 Method. Bone age estimation is crucial for development status evaluation in the pediatric population and is widely applied in different areas, such as education, medicine, and pediatric hygiene, so the accuracy of bone age estimation outstands. G-P-based bone age estimation is performed by comparing a patient's left-hand radiograph to radiograph of standard among G-P atlas. However, the process of comparing multiple images can be repetitive and is sometimes subjective since the accuracy mainly depends on the experience of a radiologist himself or herself. Interobserver and interobserver variability was shown in practice. The TW method is to analyze a specific bone piece by piece, and it tends to be more accurate to evaluate bone age than GP, and the variability of interobserver and interobservers is less (Bull *et al.* 1999, Yildiz *et al*. 2011). The GP Atlas and TW3 Bone Age Standard are both based on samples of pediatric Caucasians. Whether they are applicable to children of various ethnicities has been a concern. Previous studies have proved ethnical differences in the growth and development of children (Roche *et al*. 1974, 1978, Zhang *et al*. 2009). Recently, in 2019, Alshamrani *et al*. (2019) proved that GP bone age evaluation method is inaccurate based on the 35 meta-analysis of children of different ethnical groups and may not be the first choice for Asian population including Chinese pediatric population. The China-05 bone age standard is based on a large number of samples of contemporary Chinese pediatric population. It adopts the TW3 scoring method, and has great reliability with validation (Shaoyan *et al*. 2006). In recent years, the development of deep learning with convolutional neural networks encourages many artificial intelligence systems for bone age determination with different algorithms and models to improve the accuracy of bone age evaluation. In this paper, dataset distribution and labeling accuracy is the main focus to improve accuracy of the automatic software system for bone age determination, considering room for image classification improvement is limited (Thompson *et al*. 2020). This research is to establish an automatic software system using deep learning and artificial intelligence for bone age evaluation, based on China-05 standard (TW3-C and RUS-CHN). AI-China-05 aims to provide accurate bone age determination for Chinese pediatric population (Dai *et al*. 2021a, Ebrahimi *et al*. 2021, Hashemi *et al*. 2021, Hou *et al*. 2021, Huang *et al*. 2021b, c, Jiao *et al*. 2021, Liu *et al*. 2021a, d, Ma *et al*. 2021, Moradi *et al*. 2021, Najaafi *et al*. 2021, Shariati *et al*. 2021, Wu and Habibi 2021, Xu *et al*. 2021, Zhao *et al*. 2021b, Yu *et al*. 2022).

*Corresponding author, Ms.,
E-mail: y_chuangao@aliyun.com

ISSN: 2287-237X (Print), 2287-2388 (Online)

2. Materials and methods

2.1 Patients

20394 images from children who underwent left-hand radiography were collected, among which 1393 images are from skeletal development survey of six-tier cities of 1998 and 5994 images are from skeletal development survey of fifth-tier cities in 2005. All children are healthy population of Han ethnicity aged from 2 years old to 18 years old. The remaining 13007 radiographies are from researches on file. Since surveys of 1988 and 2005 used conventional X-ray films, a Vidar medical digital scanner (Hemdon, USA) was used to digitize the film at 150dpi and 12 bits per pixel and save it in tiff format. All X-ray films in the data set are removed from the information of gender, date of birth and filming date (Zhou *et al*. 2018, Ghazanfari *et al*. 2020, He *et al*. 2020a, b, Li *et al*. 2020a, Wang *et al*. 2020a, Dong *et al*. 2021, Liu *et al*. 2021c, Lv *et al*. 2021a, b, c, Wu *et al*. 2021, Zhao *et al*. 2021a, Zheng *et al*. 2021, Zhong *et al*. 2021, Wang *et al*. 2022, Zhang *et al*. 2022).

1020 sheets are randomly selected from the data set as the test set to evaluate the reliability of automatic software system for bone age determination. Test set is not used in model training. The remaining 19374 training set is used by hierarchical K-fold cross-validation method to train and validate the automatic software system model for bone age determination (Raschka 2015). Clinical test set composes of 400 radiographs (with patients aged from 4 to18 years old) from bone age researches on file (Azimi *et al*. 2016, Ebrahimi and Shafiei 2016, Ghadiri and Shafiei 2016a, b, c, Ghadiri *et al*. 2016a, b, c, d, Shafiei *et al*. 2016a, b, c, d, e, f, g), Clinical test set 2 has 1338 radiographs (with patients aged from 1 to 18 years old) from a clinic of department of radiology at Anhui Provincial Children's Hospital from January to August in 2020. Data for clinical test set is not used in training set (Moayedi *et al*. 2020a, b, Oyarhossein *et al*. 2020, Shariati *et al*. 2020a, Zhou *et al*. 2020a, Dai *et al*. 2021b, Guo *et al*. 2021a, b, Huang *et al*. 2021a, Huo *et al*. 2021, Liu *et al*. 2021b, Peng *et al*. 2021, Shao *et al*. 2021, Zhang *et al*. 2021a, b, c, d).

2.2 Bone development stage marking

China-05 with RUS-CHN is a new method based on the TW3-RUS bone development stage with some more stages added. Therefore, it can be converted to the TW3-C RUS bone development stage after removing the added stage (Ebrahimi and Shafiei 2017, Ebrahimi *et al*. 2017, Ehyaei *et al*. 2017, Ghadiri *et al*. 2017a, b, c, d, e, Mirjavadi *et al*. 2017a, b, c, d, Shafiei and Kazemi 2017a, b, Shafiei *et al*. 2017a, b, c, d, 2019, 2020, Shivanian *et al*. 2017, Azimi *et al*. 2018, Shafiei and She 2018).

A specific software system for data labeling was developed. 3 experienced radiologists trained by China-05 Bone Age Research Group independently label the bone development level of each radiograph. If the bone development stages presented by the 3 reviewers are exactly the same, the stage is considered correct, for the bone development stages that are not completely consistent, they will be handed over to the China-05 bone age standard maker for estimation. Before labeling, the consistency and concordance of estimations from 3 reviewers were testified. Each reviewer independently read 61 radiographs (with children aged from 2 to 18 years old). Same process is repeated after 30 days. The test results are shown in Table 1. Reviewer 1 estimates two clinical test sets and mark the bone development stage of each radiograph (Fazaeli *et al*. 2016, Ghazanfari *et al*. 2016, Habibi *et al*. 2016, 2018, Hosseini *et al*. 2018, Alipour *et al*. 2020, Cheshmeh *et al*. 2020, Ghabussi *et al*. 2020, Ghazanfari *et al*. 2020, Li *et al*. 2020a, b, Liu *et al*. 2020a, b, Moayedi *et al*. 2020c, Shariati

Table 1 Interobserver and interobserver reliability of estimation using RUS-CHN method

	Radiologist	Percentage agreement of ratings	Systematic error (years)	Random error (years)
Interobserver	1-4	81.3	0.08 a	±0.46
	2-4	81.8	-0.07	±0.43
	3-4	81.3	0.01	±0.56
	1-2	81.0	0.14b	±0.51
	1-3	81.4	0.07	±0.61
	2-3	80.1	-0.08	±0.59
Interobserver	1	91.8	0.02	±0.30
	2	89.0	0.00	±0.34
	3	84.7	0.01	±0.48
	4	89.4	-0.03	±0.40

Table 2 Bone age dataset distribution by RUS-CHN

Bone age	Training set and validation set	Test set
0~	5	1
1~	58	3
2~	228	10
3~	367	13
4~	1147	45
5~	1158	37
6~	1212	49
7~	1256	54
8~	1141	52
9~	1504	74
10~	1424	69
11~	1924	94
12~	1366	60
13~	1579	106
14~	798	49
15~	1154	85
16~	1084	67
17~	591	41
18	1378	111
In total of	19374	1020

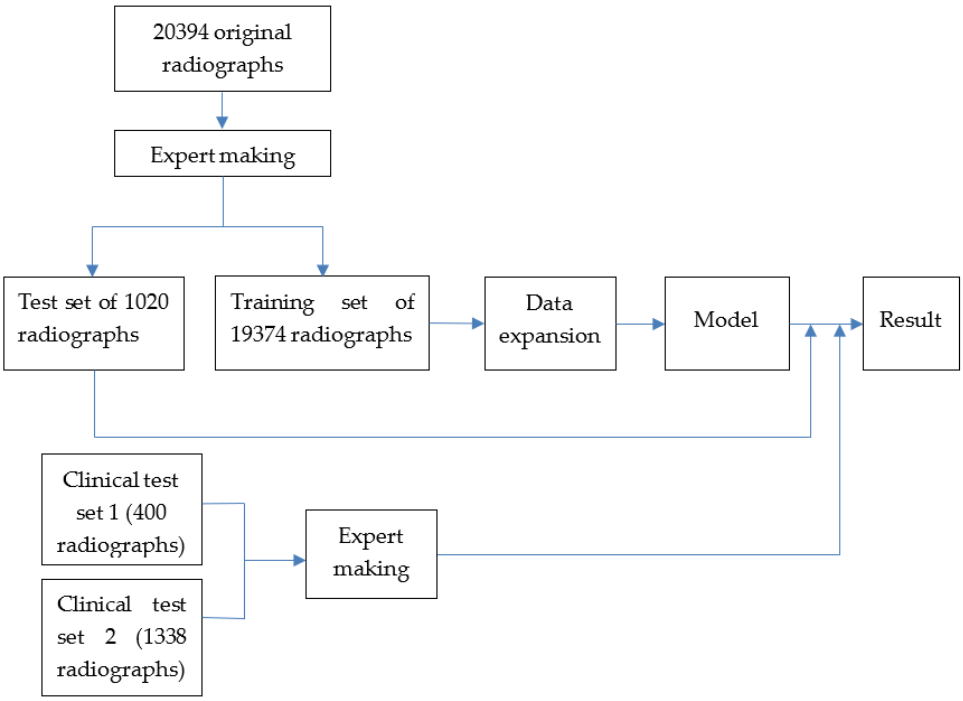

Fig. 1 Data processing flow

et al. 2020b, Shi *et al*. 2020, Wang *et al*. 2020b).

Reviewer 1, 2, and 3 are experienced radiologist, and reviewer 4 is the China-05 Bone Age Standard maker

Paired t-test was used to compare the mean difference of bone ages among interobserver and interobserver, [a] $P<0.05$, [b] $P<0.01$.

Interobserver percentage agreement of ratings is 80.0%~ 81.8%, system error -0.08~ 0.14 years old, and the random error is ±0.43~ ±0.61 years old. Interobserver percentage agreement of ratings is 84.7% ~ 91.8%, system error 0.00~ 0.02 years old, and the random error is ±0.30~ ±0.48 years old.

2.3 Data distribution

Deep learning model is mainly used for epiphyseal detection and bone development stage evaluation. Since gender information was removed when collecting the data set, all radiographs in this study were evaluated as male. Training set and test set grouped by bone age are shown in Table 2.

2.4 Training details

The original radiograph has three storage formats: dicom, png, and tiff. The three original images are all processed and transferred using open CV software into 8-bit grayscale images. Radiograph definition is enhanced by using ACE algorithm and CLAHE algorithm respectively. Complete data processing flow is shown in Fig. 1.

2.4.1 Epiphyseal detection training

Extract 7750 X-rays from the training set and use the LabelImg tool to mark the circumscribed rectangles of the 13 RUS epiphyses and the circumscribed rectangles of the hand contours. Data augmentation is carried out by adding Gaussian noise, salt and pepper noise, adjusting brightness, contrast, resolution, random translation and rotation to increase the diversity of the positioning training set (Fig. 2).

SSD and M2Det network were used in epiphyseal detection training. First, build an SSD network with mobile backbone (Fig. 3(a)), which is mainly used to identify the positioning information of the hand and radius and ulna. Batch-size is set as 32 and sent to SSD network. Data loss was calculated through output results with parameters of the model updated accordingly, and loop iteration was adopted until the validation set loss no longer drops. The loss function of the SSD algorithm is divided into two parts: calculating the confidence loss of the corresponding default box and the target category, and location loss. The overall loss is shown in Fig. 3(a).

In the SSD model, a radiograph is rotated by 90 degrees, 180 degrees, and 270 degrees, and sent to the model together with the original radiograph for identification. The hand, radius and ulna have the highest confidence as the forehand position, and according to the relative position of the radius and ulna, backhand position was turned into the forehand position and the circumscribed rectangle of the hand from the original image was cut off.

Hand radiographs cut in the previous step was used to train the M2Det (Zhao *et al*. 2019) network (Fig. 3(b)) for precise positioning. In this process, set M2Det as a single-channel input, thereby reducing the amount of calculation, improving the image feature recognition rate and processing speed, ResNet model was used for backbone to improve the accuracy of feature extracted. Confidence loss and location loss were calculated in this loss functions, and the overall loss changes of the training set and the validation set are shown in Fig. 4(b).

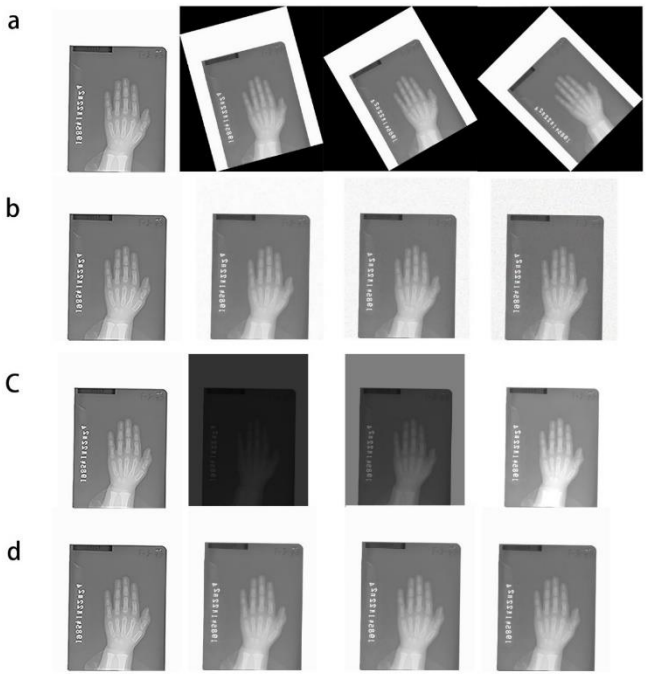

Fig. 2 The expansion method and parameters for part of the data in positioning training. (a) Randomly rotate (original film, 15°, 30°, 45°), (b) Increase salt and pepper noise (original film, 0.001, 0.01, 0.02), (c) Adjust brightness (original film, 0.2, 0.5, 1.2), (d) Adjust the contrast (original film, 0.1, 0.8, 1.5)

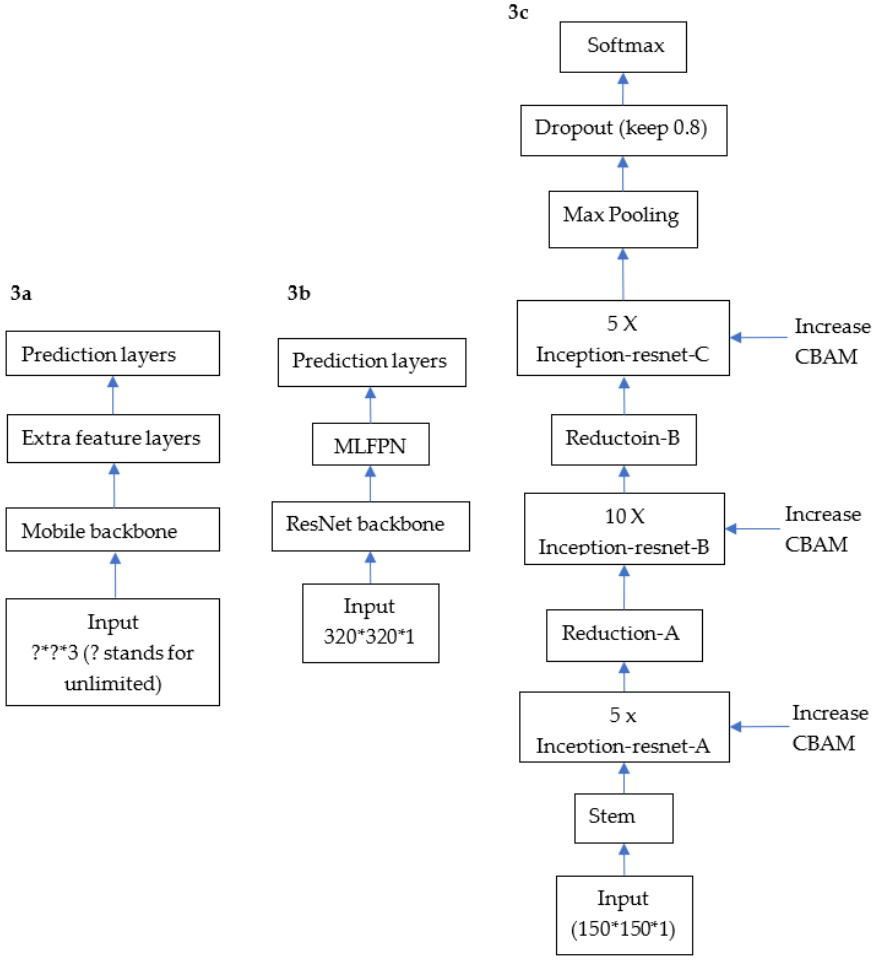

Fig. 3 Model network structure is used (a) SSD network, (b) M2Det network, (c) Inception-ResNet-V2 network)

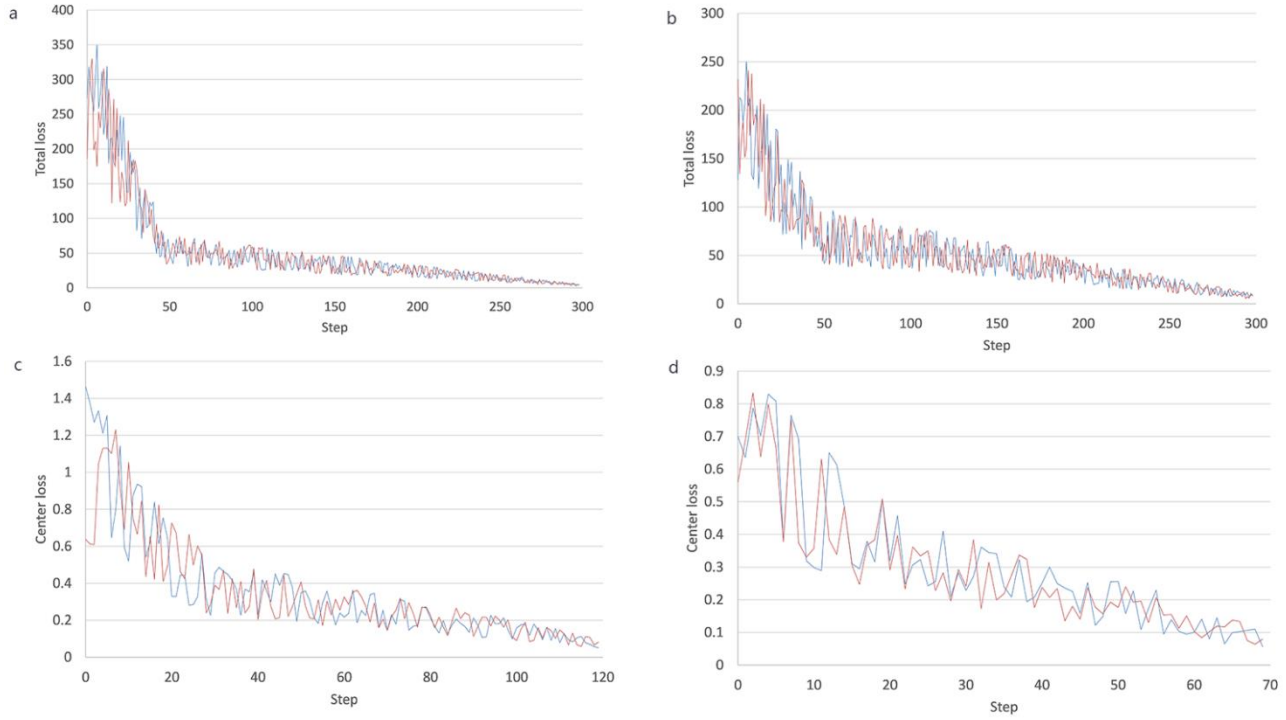

Fig. 4 (a) Total loss during training of SSD model, (b) Total loss during training of M2Det model, (c) Loss changes in training set and validation set during classification training of radius, (d) Loss changes in training set and validation set during classification training of ulna

Fig. 5 SSD and M2Det models are used to locate 13 epiphyses

2.4.2 Classification

Inception-ResNet-V2 deep learning network (Szegedy *et al*. 2017) is used in classification training. In the last pooling layer of inception-ResNet-V2, max-pooling is used to extract more epiphyseal edge features, and convolution attention mechanism module (CBAM) is used to improve the classification performance of the model (Woo *et al*. 2018), and the modified version is shown in Fig. 3(c).

Epiphyseal detection model obtained from training is used to cut out 13 epiphyses in each radiograph of the training set and process them into images of equal size, using random translation (0~75 pixels), rotation (-30°~30°), cutting, erasing, flipping, and twisting to expand to 135618 radiographs (Fig. 6). Radiographs with bone development stages inconsistent with the original ones after the expansion are eliminated. Radiographs were extracted randomly from the remaining ones for classification training.

Radius with the most detailed level to learn more bone maturity characteristics was first trained. One-hot encoding for the epiphyseal level of all training samples is used. Center loss was used as the loss function, and hierarchical K-fold method was used in the training process. The maximum number of cycles is set to 200, and early stop is

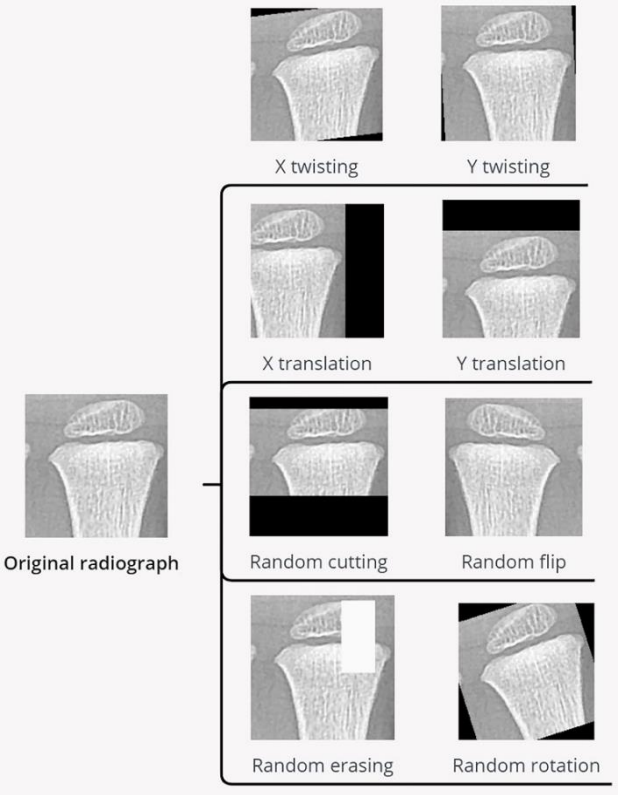

Fig. 6 Part of the expansion method in positioning training

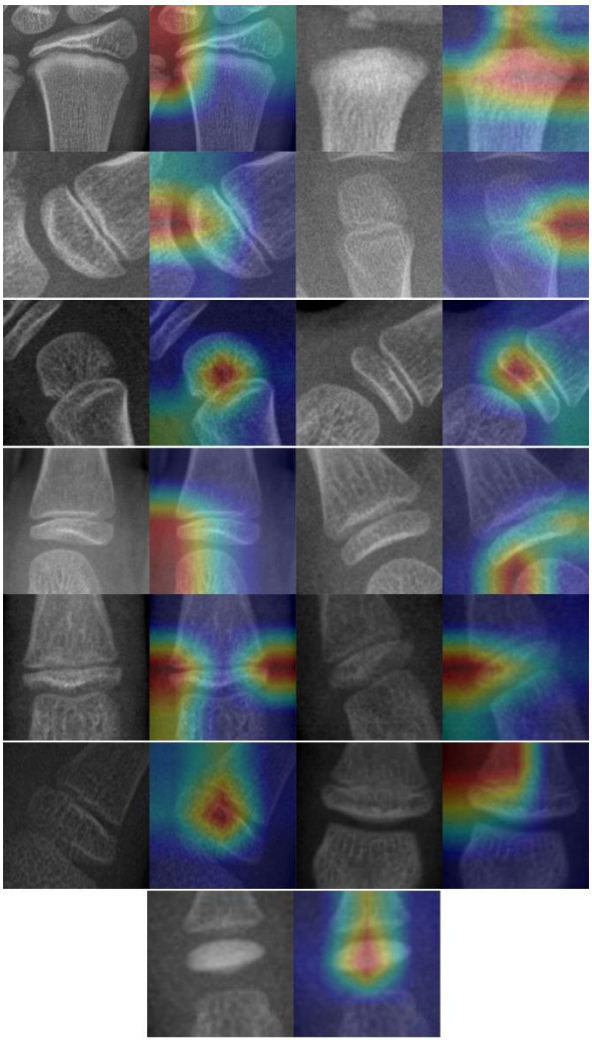

Fig. 7 The heatmap for epiphyseal classification training, similar to the features of artificial method (left is the original radiograph, and the right is the heatmap)

used. If the loss in the validation set is less than 0.01 in 6 cycles, training shall be terminated ahead of time. The hyperparameters of validation set are adjusted for the best network model, and then the remaining 12 epiphyses are trained through transfer training. Comparing the loss changes in training process of the radius and ulna, it can be found that the training speed is accelerated by transfer training. The loss during training is shown in Figs. 4(c) and 4(d).

2.5 Experimental environment

Hardware environment: CPU: Intel 7700K, CPU: Nvidia 1080ti. Software environment: Ubuntu 16.04, tensor flow 1.5, keras 2.1.3, python3.7, open CV, LabelImg

2.6 Statistical analysis

In order to compare the performance of the automatic system for bone age evaluation, AI-China-05 with other research literatures, mean absolute difference (MAD) and the root mean square (RMS) between AI-China-05 bone age evaluation system and artificial bone age evaluation to evaluate the performance of automatic software system for bone age evaluation (Larson *et al*. 2018), Percentage of radiographs with difference between AI-China-05 bone age and artificial evaluation bone age within ±0.5 years (including 0.5 years) is calculated to evaluate bone age accuracy (Omidi *et al*. 2013, Ghadiri *et al*. 2016d).

Percentage agreement and accuracy rate between AI-China-05 bone development stage and the artificial evaluation stage of each bone age in the test set are calculated to evaluate the accuracy of AI-China-05 on different age stages. Systematic error is mean difference between AI-China-05 bone age and artificial evaluation bone age, and random error is age difference of 95% confidence interval (Acheson *et al*. 1966). Statistical analysis was performed by using SPSS 26.0 software.

Since TW3-C RUS method uses the fusion of the radius and ulnar epiphyses as the end of bone age evaluation, the maximum bone age obtained is 16.5 years old for male cohort and 15 years old for female cohort. Mature age of the wrist bone by RUS-CHN method is 18 years old for male cohort and 17 years old for female cohort. Therefore, the statistical range of the results of RUS-CHN method in this research is 0~ 18 years old, and the statistical range of results of TW3-C RUS method is 0~ 16.5 years old.

3. Results

None of the 1,020 radiographs in the test set and 400 radiographs in the clinical test set 1 was rejected, and two of the 1338 radiographs in the clinical test set 2 were rejected

Table 3 Percentage agreement and accuracy rate of bone development stage with bone age artificial estimation stage

Bone age (year)	n	RUS-CHN		TW3-C RUS	
		Percentage agreement of ratings	Bone age accuracy rate	Percentage agreement of ratings	Bone age accuracy rate
0~	14	87.9	100.0	85.5	100.0
3~	13	91.1	92.3	90.1	100.0
4~	45	97.3	100.9	95.6	95.1
5~	37	89.4	91.9	85.6	92.3
6~	49	83.8	81.6	85.9	77.5
7~	54	84.9	94.4	89.3	86.7
8~	52	86.2	96.2	90.6	95.8
9~	74	82.5	93.2	89.3	90.8
10~	69	77.3	95.6	84.6	79.7
11~	94	78.5	96.8	89.4	93.1
12~	60	70.6	100.0	82.3	98.2
13~	106	76.6	100.0	85.4	99.1
14~	49	81.2	93.9	86.5	96.1
15~	85	89.6	96.5	87.3	89.2
16~	67	94.1	80.6	97.6	97.3
17~	41	96.4	78.0	--	--
18	111	99.4	93.7	--	--
average	1020	85.6	93.7	90.9	93.2

Table 4 Discrepancy, MAD and RMS between bone age determined by AI-China-05 and bone age of artificial determination

Evaluation index	RUS-CHN	TW3-C RUS
System error	0.04	0.04
Random error	±0.40	±0.38
MAD	0.17	0.16
RMS	0.29	0.28

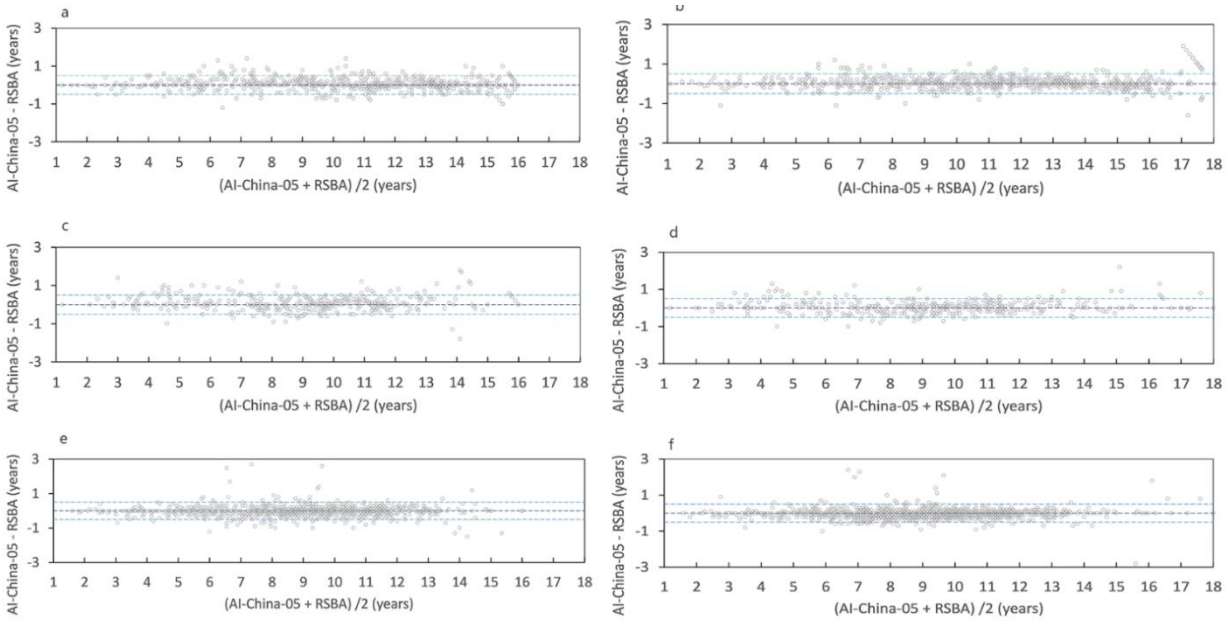

Fig. 8 Bland-Altman plots show the difference between AI-China-05 and reference standard bone age (RSBA) (a) test set with TW3-C RUS, (b) test set with RUS-CHN, (c) cliniacal test set 1 with TW3-C RUS, (d) cliniaca test set 1 with RUS-CHN, (e) clinical test set 2 with TW3-C RUS, (f) cliniancal test set 2 with RUS-CHN

Table 5 Test results of AI-China-05 (RUS-CHN and TW3-C RUS) in clinical test set

Evaluation index	Clinical test set 1 (n = 400）		Clinical test set 2 (n = 1338）	
	RUS-CHN	TW3-C RUS	RUS-CHN	TW3-C RUS
System error	0.07	0.09	-0.03	-0.03
Random error	±0.50	±0.57	±0.36	±0.38
MAD	0.25	0.28	0.14	0.15
RMS	0.36	0.41	0.26	0.27
Percentage agreement of ratings	74.4	82.5	87.2	91.9
Bone age accuracy rate (percentage)	89.3	85.3	96.4	95.7

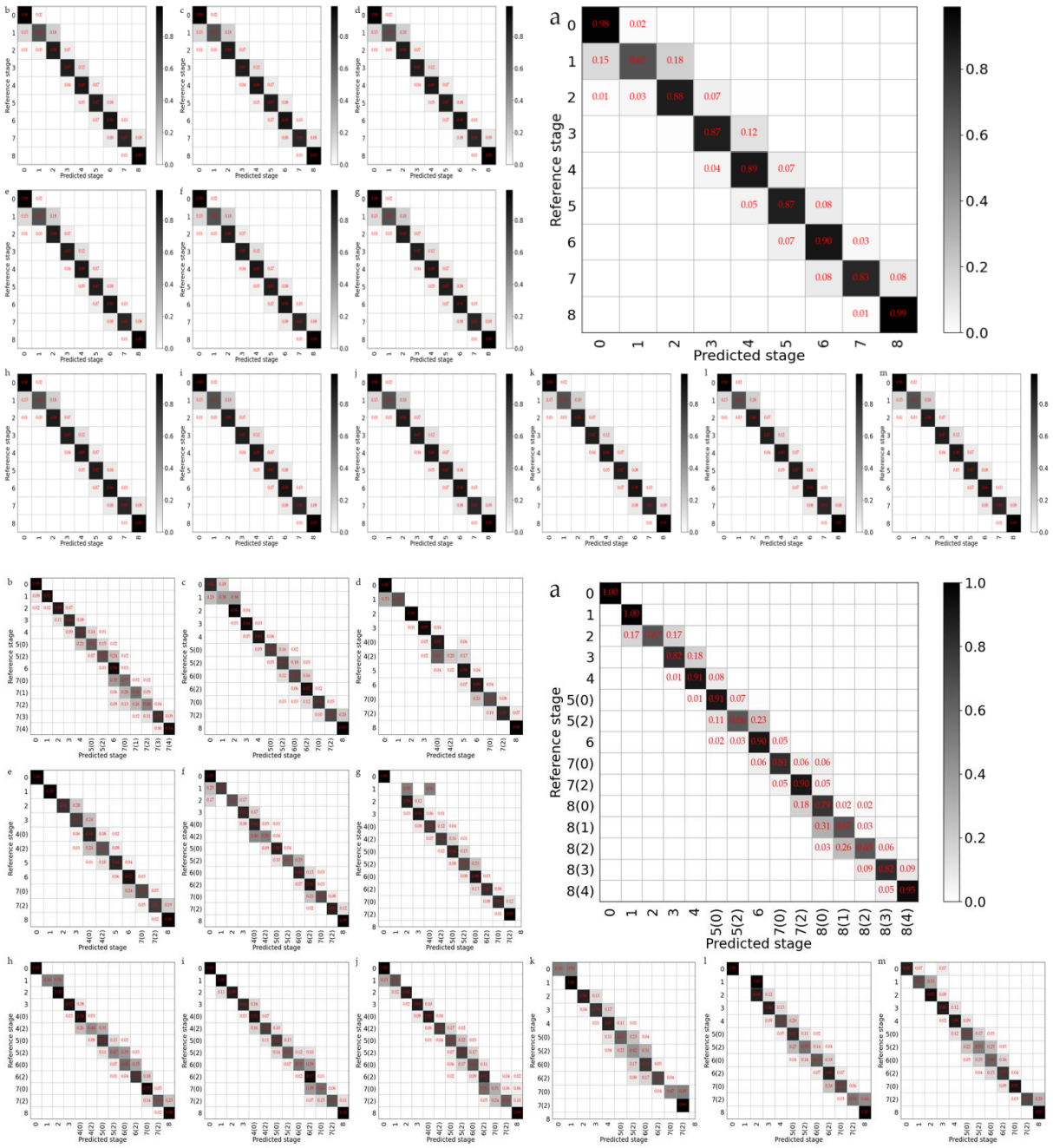

Fig. 9(1) Percentage agreement in stages between AI-China-05 (horizaontal) and reference stage (vertical) for each of the thirteen bones in the test set. (TW3-C RUS and RUS-CHN)

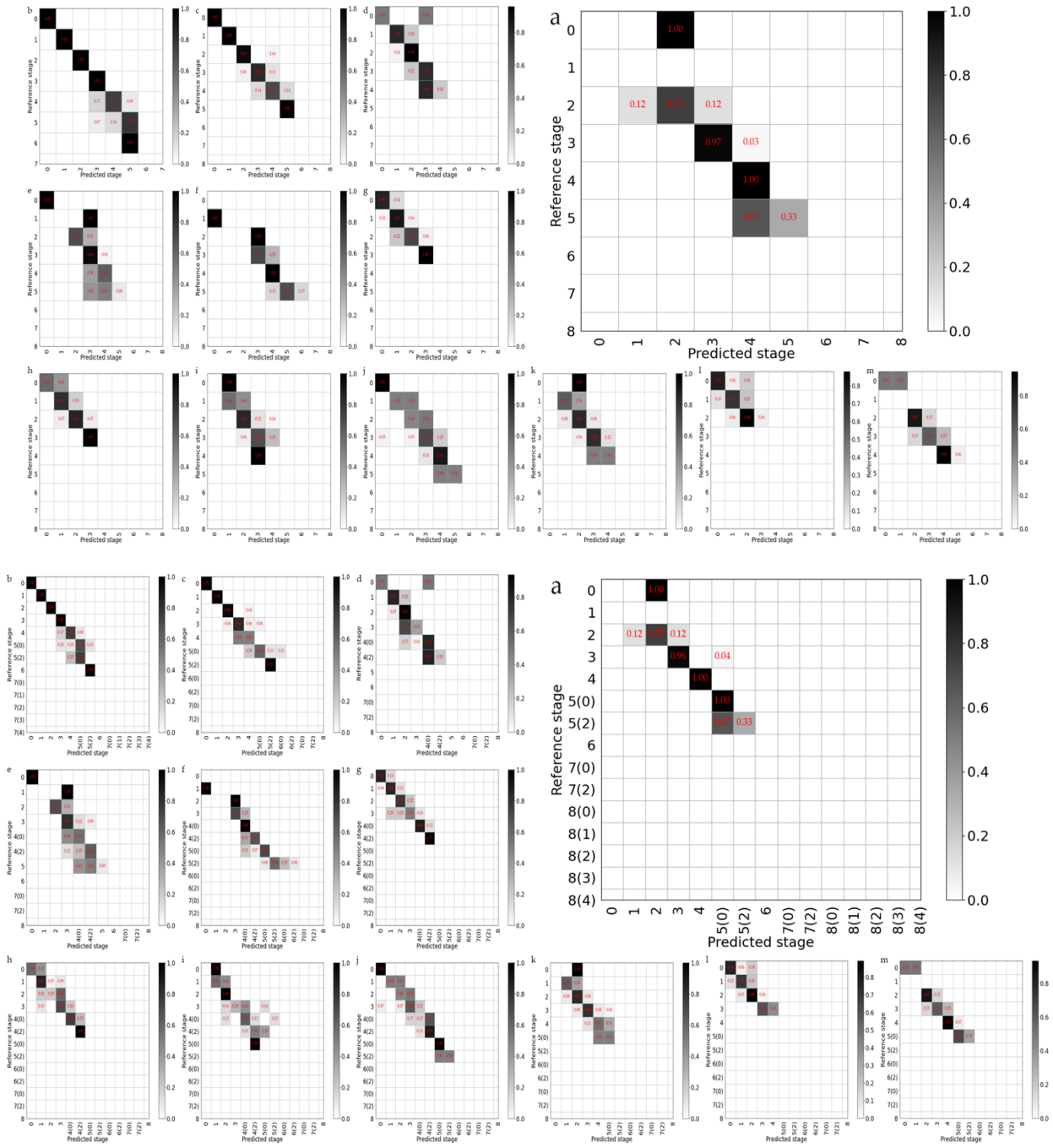

Fig. 9(2) Percentage agreement in stages between AI-China-05 (horizaontal) and reference stage (vertical) for each of the thirteen bones in the cliniacal test set 1. (TW3-C RUS and RUS-CHN)

(0.15%). 13 epiphyseal classification training heatmap is as shown in Fig. 7.

It can be seen from Table 3 that the percentage agreement of bone development level between results of AI-China-05 RUS-CHN method and artificial evaluation stage in the test set of different bone age intervals is 70.6%-99.4% (average 85.6%), and the bone age accuracy rate is 78%~ 100% (average 93.7%), AI-China-05 and TW3-C RUS methods are 82.3%~97.6% (average 90.9%) and 77.5%~100% (average 93.2%). System error and random error between AI-China-05 ‘s RUS-CHN method and TW3-C RUS method shows perfect agreement with validation test results of radiologists. Bone ages determinations of RUS-CHN and TW3-C RUS are consistent with artificial estimation of bone age that shows in MAD (0.17 and 0.16 years) and RMA (0.29 and 0.28 years). (Table 4).

Fig. 8 shows the difference between AI-China-05 between reference standard bone age (RSBA) on test set and clinical sets, which is distributed around 0, and most of them are within ±0.5 years old (bule line). The percentage agreement of bone development stages between AI-China - 05 and reference stage is displayed by confusion matrix in

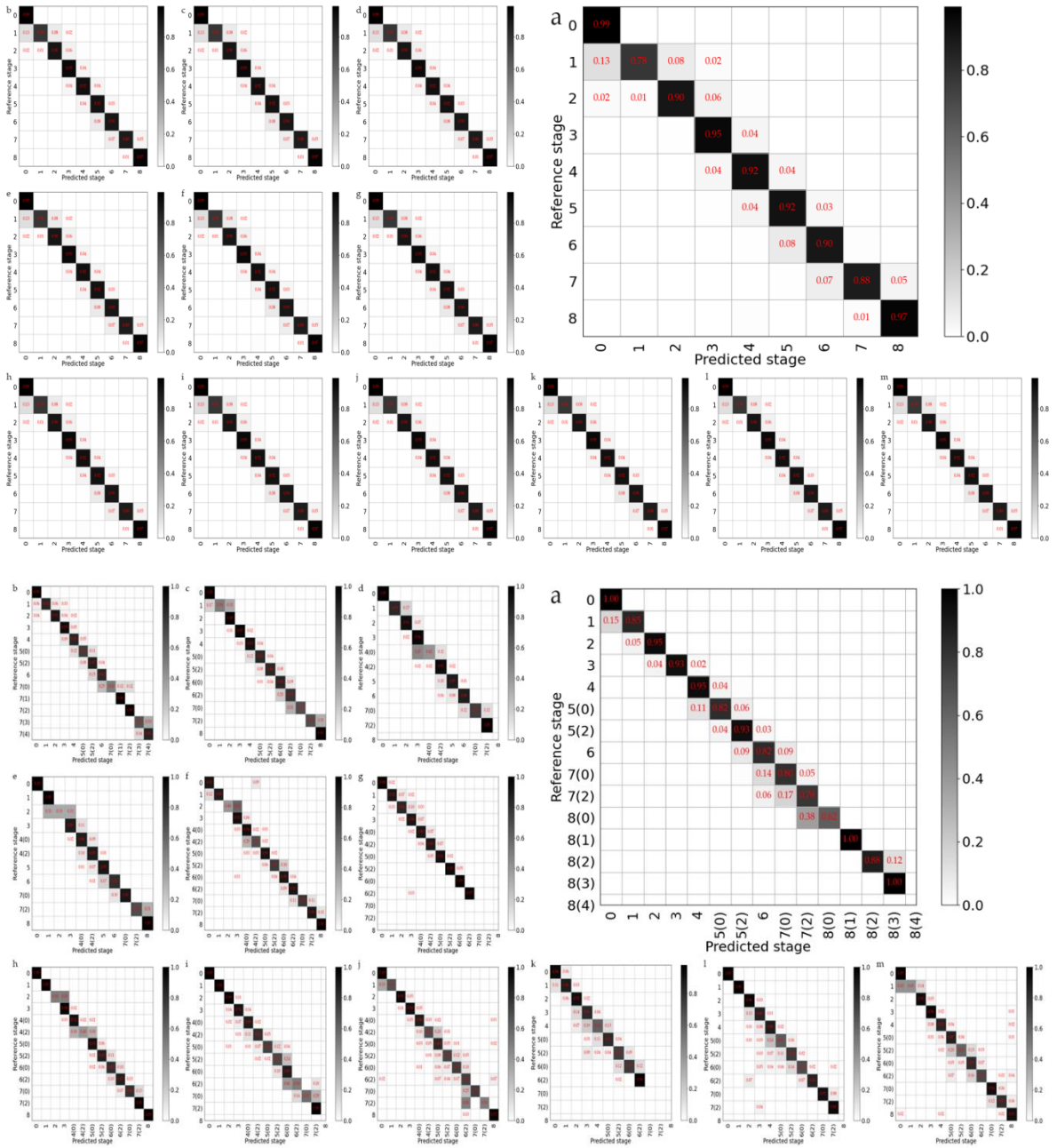

Fig. 9(3) Percentage agreement in stages between AI-China-05 (horizaontal) and reference stage (vertical) for each of the thirteen bones in the cliniacal test set 2, (TW3-C RUS and RUS-CHN), (a) Radius (b) Ulna (c) first metacarpal (d) third metacarpals (e) fifth metacarpals (f) proximal phalanx of the first finger (g) proximal phalanges of the third inger (h) proximal phalanges of the fifth finger (i) midddle phalanges of the third fingers (j) midddle phalanges of the fifth fingers (k) distal phlanx of the first finger (l) distal phlanx of the third finger (m) distal phlanx of the fifth finger

Figs. 9(1)-9(3). Test index of two separate clinical test sets shows a lower concordance rate in AI-China-05 of clinical test set 1 with reference age and a slightly higher concordance rate with reference age.

4. Conclusions

Two major left-hand wrist radiograph-based methods are currently used for bone age estimation: the Greulich-Pyle (GP) and Tanner-Whitehouse (TW) methods. There are two factors that affect the estimation the most. The first factor is the reliability of evaluation method of bone age marking. Research shows that GP method tends to be subjective compared with a complete radiograph. For example, the study of Bull *et al.* (1999) found that in clinical practice, the average bone age difference of repeated evaluations of GP atlas was 0.14±1.16 years (range from 2.46 to 2.18 years), while the average bone age difference using TW method was 0.01±0.71 years old (range from 2.46 to 2.18 years old). The second one is the reliability or professionalism of the reviewer that labeling

Table 6 Comparison of MAD, RMS and other automatic system for bone age determination in testset

Author	Marking method	MAD (year)	RMS (year)
AL-China-05 RC method	China-05	0.17	0.29
AL-China-05 TW3-C RUC method	China-05	0.16	0.28
BoneXpert (Zhang *et al*. 2013)	GP, TW3	--	Male cohort 0.64, Female cohort 0.68
RSNA Pediatric Bone Age Machine Learning Challenge (Halabi *et al*. 2018)	GP	0.35~0.38 (Top 6)	--
Zhou *et al*. (2020b)	TW3	--	0.50
Son *et al*. (2019)	TW3	0.46	0.62

MAD mean absolute difference, RMS, root mean square difference, GP, Greulich-Pyle atlas, TW3,Tanner-Whitehouse 3

the radiographs.

In recent years, due to the rapid development of artificial intelligence (AI), especially deep learning technology has promoted automatic evaluation of bone age that has gradually been applied in practice. Automatic bone age estimation system is based on machine learning with artificial bone age evaluation as training dataset. Therefore, radiograph marking in training set is the key to realize efficiency of automatic estimation.

Research in Stanford University takes the mean value of three reviewers' estimations as the reference bone age (Ground Truth) (Larson *et al*. 2018), which narrows estimation discrepancy between different reviewers. Son *et al*. (2019) uses TW3-RUS method for bone age evaluation with bone age of consensus between two reviewers as reference bone age development stage. Some researches take mean value of bone development stage from four reviewers as reference value. There are also studies using the average of the bone development stages of 4 reviewers as the reference standard (SONG *et al*. 2019). Bone age at certain age groups that are classified by obvious changes should be carefully handled and may not be suitable for continuous variable calculation. Zhou *et al*. (2020b) also uses TW3 method for automatic software system for bone age estimation. In his study, 5 from more than 100 radiologists and endocrinologists were selected. Estimation that at least 3 reviewers agreed on is used as reference bone age for each bone. However, none of these studies conducted reliability tests on reviewers that mark radiographs.

The research of Shaoyan *et al*. (2006) showed that long-term experience in bone age evaluation and participation in training help to improve the consistency of bone age evaluation. Therefore, in order to control the quality of the labeling, reliability of the three radiologists were tested before labeling (Table 1), and the test results reached or exceeded the upper limit of the reliability of the TW method international wide (international TW method reliability test shows interobserver with interobserver percentage agreement of ratings were 82.7%, ~91.4% and 74.4%~ 80.5%, random errors are ±0.42 years old~ ±0.50 years old and ±0.58 years old~ ±0.76 years old (Medicus *et al*. 1971, Beunen and Cameron 1980, Wenzel and Melsen 1982, Bull *et al*. 1999). In addition, determination of consensus among three radiologists were used for marking, and when results inconsistent, maker of China 05 Bone Age Standard makes the final decision.

In addition, a large sample size (samples from the Chinese Children's Bone Development Research Survey (CHN in 1988 and the China-05 Bone Development Survey in 2005)) are included to ensure accurate reference bone age for learning set dataset. These samples are taken from healthy population by stratified cluster sampling method

and have a relatively uniform sample distribution across a wide range of ages. Furthermore, the wrist radiograph shooting method is more standardized, which enables model to better learn and evaluate classification characteristics of bone development.

In 2019, Son *et al*. (2019) applied the deep learning of VGGNet to study the automatic software system for bone by TW3 method. This method extracts key epiphyses by locating the region of interest (ROI), but this method is subject to background interference, resulting in a reading rejection rate of 1.6%. In contrast, our system was developed according to the convolutional neural network of SSD and M2Det to position and cut key epiphyses. This method is robust to radiographs with different hand postures. Final model doesn't show failure of epiphyseal positioning.

In 2020, Zhou *et al*. (2020b) used ResNet deep learning for automatic software system for bone age estimation. Inception-ResNet-V2 model with 164 layers and 54.3M parameters is used in this study. This model has wider and deeper structural features than the ResNet model, so that it can better learn bone maturity characteristics with more complex expressions. Radiographs that are inconsistent with the original bone development level are eliminated to guarantee that proper bone development maturity characteristics shall be used for model to learn, thereby improving the classification accuracy.

Therefore, the AI-China-05 bone age performance is improved by controlling the quality of marking, appropriate data set samples, and improving the deep learning model. Compared with other automatic system for bone age estimation, MAD and RMS are both improved.

This study had several limitations. First, each epiphysis uses an independent classification model, which takes up more hardware resources. In addition, the model in this paper has not yet been able to identify certain normal physiological variations in the bone development of the wrist, such as Brachydactyly type A3 (BDA3), which occurs in different populations between 3.4% and 21.0%. The incidence is higher in Asian population (Guo *et al*. 2012). Recognition of phalanx deformities by the deep

learning model will improve the accuracy of automatic software system for bone age estimation, which will be the focus of further study.

References

Acheson, R.M., Vicinus, J.H. and Fowler, G.B. (1966), "Studies in the reliability of assessing skeletal maturity from x-rays: Part III. Greulich-Pyle Atlas and Tanner-Whitehouse method contrasted", *Human Biol*., 204-218.

Alipour, M., Torabi, M.A., Sareban, M., Lashini, H., Sadeghi, E., Fazaeli, A., Habibi, M. and Hashemi, R. (2020), "Finite element and experimental method for analyzing the effects of martensite morphologies on the formability of DP steels", *Mech. Based Des. Struct.*, **48**(5), 525-541. https://doi.org/10.1080/15397734.2019.1633343.

Alshamrani, K., Messina, F. and Offiah, A.C. (2019), "Is the Greulich and Pyle atlas applicable to all ethnicities? A systematic review and meta-analysis", *Eur. Radiol.*, **29**(6), 2910-2923. https://doi.org/10.1007/s00330-018-5792-5.

Azimi, M., Mirjavadi, S.S., Shafiei, N. and Hamouda, A.M.S. (2016), "Thermo-mechanical vibration of rotating axially functionally graded nonlocal Timoshenko beam", *Appl. Phys. A*, **123**(1), 104. https://doi.org/10.1007/s00339-016-0712-5.

Azimi, M., Mirjavadi, S.S., Shafiei, N., Hamouda, A.M.S. and Davari, E. (2018), "Vibration of rotating functionally graded Timoshenko nano-beams with nonlinear thermal distribution", *Mech. Adv. Mater. Struct.*, **25**(6), 467-480. https://doi.org/10.1080/15376494.2017.1285455.

Beunen, G. and Cameron, N. (1980), "The reproducibility of TW2 skeletal age assessments by a self-taught assessor", *Annal. Human Biol.*, **7**(2), 155-162. https://doi.org/10.1080/03014468000004181.

Bull, R.K., Edwards, P.D., Kemp, P.M., Fry, S. and Hughes, I.A. (1999), "Bone age assessment: a large scale comparison of the Greulich and Pyle, and Tanner and Whitehouse (TW2) methods", *Arch. Dis. Child.*, **81**(2), 172-173. https://doi.org/10.1136/adc.81.2.172.

Cheshmeh, E., Karbon, M., Eyvazian, A., Jung, D.w., Habibi, M. and Safarpour, M. (2020), "Buckling and vibration analysis of FG-CNTRC plate subjected to thermo-mechanical load based on higher order shear deformation theory", *Mech. Based Des. Struct.*, 1-24. https://doi.org/10.1080/15397734.2020.1744005.

Dai, Z., Jiang, Z., Zhang, L. and Habibi, M. (2021a), "Frequency characteristics and sensitivity analysis of a size-dependent laminated nanoshell", *Adv. Nano Res.*, **10**(2), 175-189. https://doi.org/10.12989/ANR.2021.10.2.175.

Dai, Z., Zhang, L., Bolandi, S.Y. and Habibi, M. (2021b), "On the vibrations of the non-polynomial viscoelastic composite open-type shell under residual stresses", *Compos. Struct.*, **263**, 113599. https://doi.org/10.1016/j.compstruct.2021.113599.

Dong, J., Cong, Y., Sun, G., Fang, Z. and Ding, Z. (2021), "Where and how to transfer: Knowledge aggregation-induced transferability perception for unsupervised domain adaptation", *IEEE T. Pattern Anal.*, 1-1. https://doi.org/10.1109/TPAMI.2021.3128560.

Ebrahimi, F. and Shafiei, N. (2016), "Application of Eringen's nonlocal elasticity theory for vibration analysis of rotating functionally graded nanobeams", *Smart Struct. Syst.*, **17**(5), 837-857. https://doi.org/10.12989/sss.2016.17.5.837.

Ebrahimi, F. and Shafiei, N. (2017), "Influence of initial shear stress on the vibration behavior of single-layered graphene sheets embedded in an elastic medium based on Reddy's higher-order shear deformation plate theory", *Mech. Adv. Mater. Struct.*, **24**(9), 761-772. https://doi.org/10.1080/15376494.2016.1196781.

Ebrahimi, F., Shafiei, N., Kazemi, M. and Mousavi Abdollahi, S.M. (2017), "Thermo-mechanical vibration analysis of rotating nonlocal nanoplates applying generalized differential quadrature method", *Mech. Adv. Mater. Struct.*, **24**(15), 1257-1273. https://doi.org/10.1080/15376494.2016.1227499.

Ebrahimi, F., Mohammadi, K., Barouti, M.M. and Habibi, M. (2021), "Wave propagation analysis of a spinning porous graphene nanoplatelet-reinforced nanoshell", *Wave. Random Complex.*, **31**(6), 1655-1681. https://doi.org/10.1080/17455030.2019.1694729.

Ehyaei, J., Akbarshahi, A. and Shafiei, N. (2017), "Influence of porosity and axial preload on vibration behavior of rotating FG nanobeam", **5**(2), 141-169. https://doi.org/10.12989/anr.2017.5.2.141.

Fazaeli, A., Habibi, M. and Ekrami, A.A. (2016), "Experimental and finite element comparison of mechanical properties and formability of dual phase steel and ferrite - pearlite steel with the same chemical composition %J Metallurgical Engineering", *Metall. Eng.*, **19**(2), 84-93. https://doi.org/10.22076/me.2017.41458.1064.

Ghabussi, A., Habibi, M., NoormohammadiArani, O., Shavalipour, A., Moayedi, H. and Safarpour, H. (2020), "Frequency characteristics of a viscoelastic graphene nanoplatelet–reinforced composite circular microplate", *J. Vib. Control*, **27**(1-2), 101-118. https://doi.org/10.1177/1077546320923930.

Ghadiri, M. and Shafiei, N. (2016a), "Nonlinear bending vibration of a rotating nanobeam based on nonlocal Eringen's theory using differential quadrature method", *Microsyst. Technol.*, **22**(12), 2853-2867. https://doi.org/10.1007/s00542-015-2662-9.

Ghadiri, M. and Shafiei, N. (2016b), "Vibration analysis of a nano-turbine blade based on Eringen nonlocal elasticity applying the differential quadrature method", *J. Vib. Control*, **23**(19), 3247-3265. https://doi.org/10.1177/1077546315627723.

Ghadiri, M. and Shafiei, N. (2016c), "Vibration analysis of rotating functionally graded Timoshenko microbeam based on modified couple stress theory under different temperature distributions", *Acta Astronaut.*, **121**, 221-240. https://doi.org/https://doi.org/10.1016/j.actaastro.2016.01.003.

Ghadiri, M., Hosseini, S.H.S. and Shafiei, N. (2016a), "A power series for vibration of a rotating nanobeam with considering thermal effect", *Mech. Adv. Mater. Struct.*, **23**(12), 1414-1420. https://doi.org/10.1080/15376494.2015.1091527.

Ghadiri, M., Shafiei, N. and Akbarshahi, A. (2016b), "Influence of thermal and surface effects on vibration behavior of nonlocal rotating Timoshenko nanobeam", *Appl. Phys. A*, **122**(7), 673. https://doi.org/10.1007/s00339-016-0196-3.

Ghadiri, M., Shafiei, N. and Alireza Mousavi, S. (2016c), "Vibration analysis of a rotating functionally graded tapered microbeam based on the modified couple stress theory by DQEM", *Appl. Phys. A*, **122**(9), 837. https://doi.org/10.1007/s00339-016-0364-5.

Ghadiri, M., Shafiei, N., Salekdeh, S.H., Mottaghi, P. and Mirzaie, T. (2016d), "Investigation of the dental implant geometry effect on stress distribution at dental implant–bone interface", *J. Brazil. Soc. Mech. Sci. Eng.*, **38**(2), 335-343. https://doi.org/10.1007/s40430-015-0472-8.

Ghadiri, M., Mahinzare, M., Shafiei, N. and Ghorbani, K. (2017a), "On size-dependent thermal buckling and free vibration of circular FG Microplates in thermal environments", *Microsyst. Technol.*, **23**(10), 4989-5001. https://doi.org/10.1007/s00542-017-3308-x.

Ghadiri, M., Shafiei, N. and Alavi, H. (2017b), "Thermo-mechanical vibration of orthotropic cantilever and propped cantilever nanoplate using generalized differential quadrature method", *Mech. Adv. Mater. Struct.*, **24**(8), 636-646. https://doi.org/10.1080/15376494.2016.1196770.

Ghadiri, M., Shafiei, N. and Alavi, H. (2017c), "Vibration analysis

of a rotating nanoplate using nonlocal elasticity theory", *J. Solid Mech.*, **9**(2), 319-337.

Ghadiri, M., Shafiei, N. and Babaei, R. (2017d), "Vibration of a rotary FG plate with consideration of thermal and Coriolis effects", *Steel Compos. Struct.*, **25**(2), 197-207. https://doi.org/10.12989/SCS.2017.25.2.197.

Ghadiri, M., Shafiei, N. and Safarpour, H. (2017e), "Influence of surface effects on vibration behavior of a rotary functionally graded nanobeam based on Eringen's nonlocal elasticity", *Microsyst. Technol.*, **23**(4), 1045-1065. https://doi.org/10.1007/s00542-016-2822-6.

Ghazanfari, A., Assempour, A., Habibi, M. and Hashemi, R. (2016), "Investigation on the effective range of the through thickness shear stress on forming limit diagram using a modified Marciniak–Kuczynski model", *Modares Mech. Eng.*, **16**(1), 137-143.

Ghazanfari, A., Soleimani, S.S., Keshavarzzadeh, M., Habibi, M., Assempuor, A. and Hashemi, R. (2020), "Prediction of FLD for sheet metal by considering through-thickness shear stresses", *Mech. Based Des. Struct.*, **48**(6), 755-772. https://doi.org/10.1080/15397734.2019.1662310.

Guo, Y., Liang, H. and Deng, H. (2012), "Advances in the molecular genetics of brachydactyly", *Yi Chuan = Hereditas*, **34**(12), 1522-1528. https://doi.org/10.3724/sp.j.1005.2012.01522.

Guo, J., Baharvand, A., Tazeddinova, D., Habibi, M., Safarpour, H., Roco-Videla, A. and Selmi, A. (2021a), "An intelligent computer method for vibration responses of the spinning multi-layer symmetric nanosystem using multi-physics modeling", *Eng. Comput.*, 1-22. https://doi.org/10.1007/s00366-021-01433-4.

Guo, Y., Mi, H. and Habibi, M. (2021b), "Electromechanical energy absorption, resonance frequency, and low-velocity impact analysis of the piezoelectric doubly curved system", *Mech. Syst. Signal Proc.*, **157**, 107723. https://doi.org/10.1016/j.ymssp.2021.107723.

Habibi, M., Hashemi, R., Ghazanfari, A., Naghdabadi, R. and Assempour, A. (2016), "Forming limit diagrams by including the M–K model in finite element simulation considering the effect of bending", *Proceedings of the Institution of Mechanical Engineers, Part L: Journal of Materials: Design and Applications*. **232**(8), 625-636. https://doi.org/10.1177/1464420716642258.

Habibi, M., Hashemi, R., Fallah Tafti, M. and Assempour, A. (2018), "Experimental investigation of mechanical properties, formability and forming limit diagrams for tailor-welded blanks produced by friction stir welding", *J. Manuf. Proc.*, **31**, 310-323. https://doi.org/10.1016/j.jmapro.2017.11.009.

Halabi, S.S., Prevedello, L.M., Kalpathy-Cramer, J., Mamonov, A.B., Bilbily, A., Cicero, M., Pan, I., Pereira, L.A., Sousa, R.T., Abdala, N., Kitamura, F.C., Thodberg, H.H., Chen, L., Shih, G., Andriole, K., Kohli, M.D., Erickson, B.J. and Flanders, A.E. (2018), "The RSNA pediatric bone age machine learning challenge", *Radiology*. **290**(2), 498-503. https://doi.org/10.1148/radiol.2018180736.

Hashemi, H.R., Alizadeh, A.a., Oyarhossein, M.A., Shavalipour, A., Makkiabadi, M. and Habibi, M. (2021), "Influence of imperfection on amplitude and resonance frequency of a reinforcement compositionally graded nanostructure", *Wave. Random Complex.*, **31**(6), 1340-1366. https://doi.org/10.1080/17455030.2019.1662968.

He, S., Guo, F., Zou, Q. and HuiDing (2020a), "MRMD2.0: A python tool for machine learning with feature ranking and reduction", *Curr. Bioinform.*, **15**(10), 1213-1221. https://doi.org/10.2174/1574893615999200503030350.

He, Y., Dai, L. and Zhang, H. (2020b), "Multi-branch deep residual learning for clustering and beamforming in user-centric network", *IEEE Commun. Lett.*, **24**(10), 2221-2225. https://doi.org/10.1109/LCOMM.2020.3005947.

Hosseini, S.M.R., Habibi, M. and Assempour, A. (2018), "Experimental and numerical determination of forming limit diagram of steel-copper two-layer sheet considering the interface between the layers", *Modares Mech. Eng.*, **18**(6), 174-181.

Hou, F., Wu, S., Moradi, Z. and Shafiei, N. (2021), "The computational modeling for the static analysis of axially functionally graded micro-cylindrical imperfect beam applying the computer simulation", *Eng. Comput.*, 1-19. https://doi.org/10.1007/s00366-021-01456-x.

Huang, X., Hao, H., Oslub, K., Habibi, M. and Tounsi, A. (2021a), "Dynamic stability/instability simulation of the rotary size-dependent functionally graded microsystem", *Eng. Comput.*, 1-17. https://doi.org/10.1007/s00366-021-01399-3.

Huang, X., Zhang, Y., Moradi, Z. and Shafiei, N. (2021b), "Computer simulation via a couple of homotopy perturbation methods and the generalized differential quadrature method for nonlinear vibration of functionally graded non-uniform micro-tube", *Eng. Comput.*, 1-18. https://doi.org/10.1007/s00366-021-01395-7.

Huang, X., Zhu, Y., Vafaei, P., Moradi, Z. and Davoudi, M. (2021c), "An iterative simulation algorithm for large oscillation of the applicable 2D-electrical system on a complex nonlinear substrate", *Eng. Comput.*, 1-13. https://doi.org/10.1007/s00366-021-01320-y.

Huo, J., Zhang, G., Ghabussi, A. and Habibi, M. (2021), "Bending analysis of FG-GPLRC axisymmetric circular/annular sector plates by considering elastic foundation and horizontal friction force using 3D-poroelasticity theory", *Compos. Struct.*, **276**, 114438. https://doi.org/10.1016/j.compstruct.2021.114438.

Jiao, J., Ghoreishi, S.M., Moradi, Z. and Oslub, K. (2021), "Coupled particle swarm optimization method with genetic algorithm for the static–dynamic performance of the magneto-electro-elastic nanosystem", *Eng. Comput.*, 1-15. https://doi.org/10.1007/s00366-021-01391-x.

Larson, D.B., Chen, M.C., Lungren, M.P., Halabi, S.S., Stence, N.V. and Langlotz, C.P. (2018), "Performance of a deep-learning neural network model in assessing skeletal maturity on pediatric hand radiographs", *Radiology*. **287**(1), 313-322. https://doi.org/10.1148/radiol.2017170236.

Li, J., Tang, F. and Habibi, M. (2020a), "Bi-directional thermal buckling and resonance frequency characteristics of a GNP-reinforced composite nanostructure", *Eng. Comput.*, 1-22. https://doi.org/10.1007/s00366-020-01110-y.

Li, Y., Li, S., Guo, K., Fang, X. and Habibi, M. (2020b), "On the modeling of bending responses of graphene-reinforced higher order annular plate via two-dimensional continuum mechanics approach", *Eng. Comput.*, 1-22. https://doi.org/10.1007/s00366-020-01166-w.

Liu, Z., Su, S., Xi, D. and Habibi, M. (2020a), "Vibrational responses of a MHC viscoelastic thick annular plate in thermal environment using GDQ method", *Mech. Based Des. Struct.*, 1-26. https://doi.org/10.1080/15397734.2020.1784201.

Liu, Z., Wu, X., Yu, M. and Habibi, M. (2020b), "Large-amplitude dynamical behavior of multilayer graphene platelets reinforced nanocomposite annular plate under thermo-mechanical loadings", *Mech. Based Des. Struct.*, 1-25. https://doi.org/10.1080/15397734.2020.1815544.

Liu, H., Shen, S., Oslub, K., Habibi, M. and Safarpour, H. (2021a), "Amplitude motion and frequency simulation of a composite viscoelastic microsystem within modified couple stress elasticity", *Eng. Comput.*, 1-15. https://doi.org/10.1007/s00366-021-01316-8.

Liu, H., Zhao, Y., Pishbin, M., Habibi, M., Bashir, M.O. and Issakhov, A. (2021b), "A comprehensive mathematical

simulation of the composite size-dependent rotary 3D microsystem via two-dimensional generalized differential quadrature method", *Eng. Comput.*, 1-16. https://doi.org/10.1007/s00366-021-01419-2.

Liu, R., Wang, X., Lu, H., Wu, Z., Fan, Q., Li, S. and Jin, X. (2021c), "SCCGAN: Style and characters inpainting based on CGAN", *Mobile Netw. Appl.*, **26**(1), 3-12. https://doi.org/10.1007/s11036-020-01717-x.

Liu, Y., Wang, W., He, T., Moradi, Z. and Larco Benítez, M.A. (2021d), "On the modelling of the vibration behaviors via discrete singular convolution method for a high-order sector annular system", *Eng. Comput.*, 1-23. https://doi.org/10.1007/s00366-021-01454-z.

Lv, Z., Li, Y., Feng, H. and Lv, H. (2021a), "Deep learning for security in digital twins of cooperative intelligent transportation systems", *IEEE T. Intell. Transp.*, 1-10. https://doi.org/10.1109/TITS.2021.3113779.

Lv, Z., Qiao, L., Hossain, M.S. and Choi, B.J. (2021b), "Analysis of using blockchain to protect the privacy of drone big data", *IEEE Netw.*, **35**(1), 44-49. https://doi.org/10.1109/MNET.011.2000154.

Lv, Z., Singh, A.K. and Li, J. (2021c), "Deep learning for security problems in 5g heterogeneous networks", *IEEE Netw.*, **35**(2), 67-73. https://doi.org/10.1109/MNET.011.2000229.

Ma, L., Liu, X. and Moradi, Z. (2021), "On the chaotic behavior of graphene-reinforced annular systems under harmonic excitation", *Eng. Comput.*, 1-25. https://doi.org/10.1007/s00366-020-01210-9.

Medicus, H., Grøn, A.M. and Moorrees, C.F.A. (1971), "Reproducibility of rating stages of osseous development. (Tanner-Whitehouse system)", **35**(3), 359-371. https://doi.org/10.1002/ajpa.1330350311.

Mirjavadi, S.S., Afshari, B.M., Shafiei, N., Hamouda, A., Kazemi, M. and Structures, C. (2017a), "Thermal vibration of two-dimensional functionally graded (2D-FG) porous Timoshenko nanobeams", *Steel Compos. Struct.*, **25**(4), 415-426. https://doi.org/10.12989/scs.2017.25.4.415.

Mirjavadi, S.S., Matin, A., Shafiei, N., Rabby, S. and Mohasel Afshari, B. (2017b), "Thermal buckling behavior of two-dimensional imperfect functionally graded microscale-tapered porous beam", *J. Therm. Stress.*, **40**(10), 1201-1214. https://doi.org/10.1080/01495739.2017.1332962.

Mirjavadi, S.S., Mohasel Afshari, B., Shafiei, N., Rabby, S. and Kazemi, M. (2017c), "Effect of temperature and porosity on the vibration behavior of two-dimensional functionally graded micro-scale Timoshenko beam", *J. Vib. Control*, **24**(18), 4211-4225. https://doi.org/10.1177/1077546317721871.

Mirjavadi, S.S., Rabby, S., Shafiei, N., Afshari, B.M. and Kazemi, M. (2017d), "On size-dependent free vibration and thermal buckling of axially functionally graded nanobeams in thermal environment", *Appl. Phys. A*, **123**(5), 315. https://doi.org/10.1007/s00339-017-0918-1.

Moayedi, H., Aliakbarlou, H., Jebeli, M., Noormohammadiarani, O., Habibi, M., Safarpour, H. and Foong, L.K. (2020a), "Thermal buckling responses of a graphene reinforced composite micropanel structure", **12**(1), 2050010. https://doi.org/10.1142/s1758825120500106.

Moayedi, H., Darabi, R., Ghabussi, A., Habibi, M. and Foong, L.K. (2020b), "Weld orientation effects on the formability of tailor welded thin steel sheets", *Thin Wall. Struct.*, **149**, 106669. https://doi.org/https://doi.org/10.1016/j.tws.2020.106669.

Moayedi, H., Ebrahimi, F., Habibi, M., Safarpour, H. and Foong, L.K. (2020c), "Application of nonlocal strain–stress gradient theory and GDQEM for thermo-vibration responses of a laminated composite nanoshell", *Eng. Comput.*, **37**(4), 3359-3374. https://doi.org/10.1007/s00366-020-01002-1.

Moradi, Z., Davoudi, M., Ebrahimi, F. and Ehyaei, A.F. (2021), "Intelligent wave dispersion control of an inhomogeneous micro-shell using a proportional-derivative smart controller", *Wave. Random Complex.*, 1-24. https://doi.org/10.1080/17455030.2021.1926572.

Najaafi, N., Jamali, M., Habibi, M., Sadeghi, S., Jung, D.w. and Nabipour, N. (2021), "Dynamic instability responses of the substructure living biological cells in the cytoplasm environment using stress-strain size-dependent theory", *J. Biomol. Struct. Dyn.*, **39**(7), 2543-2554. https://doi.org/10.1080/07391102.2020.1751297.

Omidi, S., Oskooee, M.B. and Shafiei, N. (2013), "Finite element analysis of an ultra-fine grained Titanium dental implant covered by different thicknesses of hydroxyapatite layer", *Indian J. Dentistry*, **4**(1), 1-4. https://doi.org/10.1016/j.ijd.2012.https://doi.org/10.002.

Oyarhossein, M.A., Alizadeh, A.a., Habibi, M., Makkiabadi, M., Daman, M., Safarpour, H. and Jung, D.W. (2020), "Dynamic response of the nonlocal strain-stress gradient in laminated polymer composites microtubes", *Sci. Rep.*, **10**(1), 5616. https://doi.org/10.1038/s41598-020-61855-w.

Peng, D., Chen, S., Darabi, R., Ghabussi, A. and Habibi, M. (2021), "Prediction of the bending and out-of-plane loading effects on formability response of the steel sheets", *Arch. Civil Mech. Eng.*, **21**(2), 74. https://doi.org/10.1007/s43452-021-00227-1.

Raschka, S. (2015), *Python machine learning*, Packt Publishing Ltd, Mumbai, India.

Roche, A.F., Roberts, J. and Hamill, P.V. (1974), *Skeletal Maturity of Children 6-11 Years: Racial, Geographic Area, and Socioeconomic Differentials, United States*, National Center for Health Statistics, Washington, D.C., U.S.A.

Roche, A.F., Roberts, J. and Hamill, P.V. (1978), *Skeletal Maturity of Youths 12-17 Years: Racial, Geographic Area, and Socioeconomic Differentials*, National Center for Health Statistics, Washington, D.C., U.S.A.

Shafiei, N., Kazemi, M. and Ghadiri, M. (2016a), "Comparison of modeling of the rotating tapered axially functionally graded Timoshenko and Euler–Bernoulli microbeams", *Physica E*, **83**, 74-87. https://doi.org/10.1016/j.physe.2016.04.011.

Shafiei, N., Kazemi, M. and Ghadiri, M. (2016b), "Nonlinear vibration behavior of a rotating nanobeam under thermal stress using Eringen's nonlocal elasticity and DQM", *Appl. Phys. A*, **122**(8), 728. https://doi.org/10.1007/s00339-016-0245-y.

Shafiei, N., Kazemi, M. and Ghadiri, M. (2016c), "Nonlinear vibration of axially functionally graded tapered microbeams", *Int. J. Eng. Sci.*, **102**, 12-26. https://doi.org/10.1016/j.ijengsci.2016.02.007.

Shafiei, N., Kazemi, M. and Ghadiri, M. (2016d), "On size-dependent vibration of rotary axially functionally graded microbeam", *Int. J. Eng. Sci.*, **101**, 29-44. https://doi.org/10.1016/j.ijengsci.2015.12.008.

Shafiei, N., Kazemi, M., Safi, M. and Ghadiri, M. (2016e), "Nonlinear vibration of axially functionally graded non-uniform nanobeams", *Int. J. Eng. Sci.*, **106**, 77-94. https://doi.org/10.1016/j.ijengsci.2016.05.009.

Shafiei, N., Mousavi, A. and Ghadiri, M. (2016f), "On size-dependent nonlinear vibration of porous and imperfect functionally graded tapered microbeams", *Int. J. Eng. Sci.*, **106**, 42-56. https://doi.org/10.1016/j.ijengsci.2016.05.007.

Shafiei, N., Mousavi, A. and Ghadiri, M. (2016g), "Vibration behavior of a rotating non-uniform FG microbeam based on the modified couple stress theory and GDQEM", *Compos. Struct.*, **149**, 157-169. https://doi.org/10.1016/j.compstruct.2016.04.024.

Shafiei, N. and Kazemi, M. (2017a), "Buckling analysis on the bi-dimensional functionally graded porous tapered nano-/micro-scale beams", *Aerosp. Sci. Technol.*, **66**, 1-11. https://doi.org/10.1016/j.ast.2017.02.019.

Shafiei, N. and Kazemi, M. (2017b), "Nonlinear buckling of functionally graded nano-/micro-scaled porous beams", *Compos. Struct.*, **178**, 483-492. https://doi.org/10.1016/j.compstruct.2017.07.045.

Shafiei, N., Ghadiri, M., Makvandi, H. and Hosseini, S.A. (2017a), "Vibration analysis of Nano-Rotor's Blade applying Eringen nonlocal elasticity and generalized differential quadrature method", *Appl. Math. Modell.*, **43**, 191-206. https://doi.org/10.1016/j.apm.2016.10.061.

Shafiei, N., Kazemi, M. and Fatahi, L. (2017b), "Transverse vibration of rotary tapered microbeam based on modified couple stress theory and generalized differential quadrature element method", *Mech. Adv. Mater. Struct.*, **24**(3), 240-252. https://doi.org/10.1080/15376494.2015.1128025.

Shafiei, N., Mirjavadi, S.S., Afshari, B.M., Rabby, S. and Hamouda, A.M.S. (2017c), "Nonlinear thermal buckling of axially functionally graded micro and nanobeams", *Compos. Struct.*, **168**, 428-439. https://doi.org/10.1016/j.compstruct.2017.02.048.

Shafiei, N., Mirjavadi, S.S., MohaselAfshari, B., Rabby, S. and Kazemi, M. (2017d), "Vibration of two-dimensional imperfect functionally graded (2D-FG) porous nano-/micro-beams", *Comput. Method Appl. Mech. Eng.*, **322**, 615-632. https://doi.org/10.1016/j.cma.2017.05.007.

Shafiei, N. and She, G.L. (2018), "On vibration of functionally graded nano-tubes in the thermal environment", *Int. J. Eng. Sci.*, **133**, 84-98. https://doi.org/10.1016/j.ijengsci.2018.08.004.

Shafiei, N., Ghadiri, M. and Mahinzare, M. (2019), "Flapwise bending vibration analysis of rotary tapered functionally graded nanobeam in thermal environment", *Mech. Adv. Mater. Struct.*, **26**(2), 139-155. https://doi.org/10.1080/15376494.2017.1365982.

Shafiei, N., Hamisi, M. and Ghadiri, M. (2020), "Vibration analysis of rotary tapered axially functionally graded Timoshenko nanobeam in thermal environment", *J. Solid Mech.*, **12**(1), 16-32.

Shao, Y., Zhao, Y., Gao, J. and Habibi, M. (2021), "Energy absorption of the strengthened viscoelastic multi-curved composite panel under friction force", *Arch. Civil Mech. Eng.*, **21**(4), 141. https://doi.org/10.1007/s43452-021-00279-3.

Shaoyan, Z., Zhenlie, W. and Xunzhang, S. (2006), "The standards of skeletal maturity of hand and wrist for Chinese-China 05 II. Reliability of assessing skeletal age by RUS-CHN and TW_3-C carpal methods", *Chinese J. Sports Med.*, **6**.

Shariati, A., Jung, D.w., Mohammad-Sedighi, H., Żur, K.K., Habibi, M. and Safa, M. (2020a), "On the vibrations and stability of moving viscoelastic axially functionally graded nanobeams", *Materials*, **13**(7), 1707. https://doi.org/10.3390/ma13071707.

Shariati, A., Jung, D.W., Mohammad-Sedighi, H., Żur, K.K., Habibi, M. and Safa, M. (2020b), "Stability and dynamics of viscoelastic moving rayleigh beams with an asymmetrical distribution of material parameters", *Symmetry*, **12**(4), 586. https://doi.org/10.3390/sym12040586.

Shariati, A., Habibi, M., Tounsi, A., Safarpour, H. and Safa, M. (2021), "Application of exact continuum size-dependent theory for stability and frequency analysis of a curved cantilevered microtubule by considering viscoelastic properties", *Eng. Comput.*, **37**(4), 3629-3648. https://doi.org/10.1007/s00366-020-01024-9.

Shi, X., Li, J. and Habibi, M. (2020), "On the statics and dynamics of an electro-thermo-mechanically porous GPLRC nanoshell conveying fluid flow", *Mech. Based Des. Struct.*, 1-37. https://doi.org/10.1080/15397734.2020.1772088.

Shivanian, E., Ghadiri, M. and Shafiei, N. (2017), "Influence of size effect on flapwise vibration behavior of rotary microbeam and its analysis through spectral meshless radial point interpolation", *Appl. Phys. A*, **123**(5), 329. https://doi.org/10.1007/s00339-017-0955-9.

Son, S.J., Song, Y., Kim, N., Do, Y., Kwak, N., Lee, M.S. and Lee, B.D. (2019), "TW3-based fully automated bone age assessment system using deep neural networks", *IEEE Access*, **7**, 33346-33358. https://doi.org/10.1109/ACCESS.2019.2903131.

Song, J., Gong, P., Gao, C., Han, Q., Li, X., Zhu, Z., Chen, H., Yu, Y. and Fang, X. (2019), "Construction and clinical preliminary validation of an automaticbone age assessment model based on deep learning", *Chinese J. Radiol.*, 974-978.

Szegedy, C., Ioffe, S., Vanhoucke, V. and Alemi, A.A. (2017). "Inception-v4, inception-resnet and the impact of residual connections on learning", *Proceeding of the 31st AAAI Conference on Artificial Intelligence*, California, U.S.A. February.

Thompson, N.C., Greenewald, K., Lee, K. and Manso, G.F. (2020), "The computational limits of deep learning", *arXiv preprint arXiv:2007.05558*.

Wang, T., Wei, X., Wang, J., Huang, T., Peng, H., Song, X., Cabrera, L.V. and Pérez-Jiménez, M.J. (2020a), "A weighted corrective fuzzy reasoning spiking neural P system for fault diagnosis in power systems with variable topologies", *Eng. Appl. Artif. Intell.*, **92**, 103680. https://doi.org/10.1016/j.engappai.2020.103680.

Wang, Z., Yu, S., Xiao, Z. and Habibi, M. (2020b), "Frequency and buckling responses of a high-speed rotating fiber metal laminated cantilevered microdisk", *Mech. Adv. Mater. Struct.*, 1-14. https://doi.org/10.1080/15376494.2020.1824284.

Wang, K., Wang, H. and Li, S. (2022), "Renewable quantile regression for streaming datasets", *Knowl. Based Syst.*, **235**, 107675. https://doi.org/10.1016/j.knosys.2021.107675.

Wenzel, A. and Melsen, B.J.H.b. (1982), "Replicability of assessing radiographs by the Tanner and Whitehouse-2 method", *Human Biol.*, 575-581.

Woo, S., Park, J., Lee, J.Y. and Kweon, I.S. (2018). "Cbam: Convolutional block attention module", *Proceedings of the European conference on computer vision (ECCV)*, Munich, Germany, September.

Wu, J. and Habibi, M. (2021), "Dynamic simulation of the ultra-fast-rotating sandwich cantilever disk via finite element and semi-numerical methods", *Eng. Comput.*, 1-17. https://doi.org/10.1007/s00366-021-01396-6.

Wu, X., Zheng, W., Xia, X. and Lo, D. (2021), "Data quality matters: A case study on data label correctness for security bug report prediction", *IEEE T. Softw. Eng.*, 1-1. https://doi.org/10.1109/TSE.2021.3063727.

Xu, W., Pan, G., Moradi, Z. and Shafiei, N. (2021), "Nonlinear forced vibration analysis of functionally graded non-uniform cylindrical microbeams applying the semi-analytical solution", *Compos. Struct.*, **275**, 114395. https://doi.org/10.1016/j.compstruct.2021.114395.

Yildiz, M., Guvenis, A., Guven, E., Talat, D. and Haktan, M. (2011), "Implementation and statistical evaluation of a web-based software for bone age assessment", *J. Med. Syst.*, **35**(6), 1485-1489. https://doi.org/10.1007/s10916-009-9425-z.

Yu, X., Maalla, A. and Moradi, Z. (2022), "Electroelastic high-order computational continuum strategy for critical voltage and frequency of piezoelectric NEMS via modified multi-physical couple stress theory", *Mech. Syst. Signal Proc.*, **165**, 108373. https://doi.org/10.1016/j.ymssp.2021.108373.

Zhang, S.Y., Liu, G., Ma, C.G., Han, Y.S., Shen, X.Z., Xu, R.L. and Thodberg, H.H. (2013), "Automated determination of bone age in a modern Chinese population", *Int. Scholar. Res. Notices*, **2013**, 874570. https://doi.org/10.5402/2013/874570.

Zhang, A., Sayre, J.W., Vachon, L., Liu, B.J. and Huang, H.K. (2009), "Racial differences in growth patterns of children assessed on the basis of bone age", *Radiology*, **250**(1), 228-235.

https://doi.org/10.1148/radiol.2493080468.
Zhang, B., Chen, Y.X., Wang, Z.G., Li, J.Q. and Ji, H.H. (2021a), "Influence of mach number of main flow on film cooling characteristics under supersonic condition", *Symmetry*, **13**(1), 127. https://doi.org/10.3390/sym13010127.
Zhang, L., Chen, Z., Habibi, M., Ghabussi, A. and Alyousef, R. (2021b), "Low-velocity impact, resonance, and frequency responses of FG-GPLRC viscoelastic doubly curved panel", *Compos. Struct.*, **269**, 114000. https://doi.org/10.1016/j.compstruct.2021.114000.
Zhang, X., Shamsodin, M., Wang, H., NoormohammadiArani, O., Khan, A.M., Habibi, M. and Al-Furjan, M.S.H. (2021c), "Dynamic information of the time-dependent tobullian biomolecular structure using a high-accuracy size-dependent theory", *J. Biomol. Struct. Dyn.*, **39**(9), 3128-3143. https://doi.org/10.1080/07391102.2020.1760939.
Zhang, Y., Wang, Z., Tazeddinova, D., Ebrahimi, F., Habibi, M. and Safarpour, H. (2021d), "Enhancing active vibration control performances in a smart rotary sandwich thick nanostructure conveying viscous fluid flow by a PD controller", *Wave. Random Complex.*, 1-24. https://doi.org/10.1080/17455030.2021.1948627.
Zhang, Y., Shi, X., Zhang, H., Cao, Y. and Terzija, V. (2022), "Review on deep learning applications in frequency analysis and control of modern power system", *Int. J. Electr. Power*, **136**, 107744. https://doi.org/10.1016/j.ijepes.2021.107744.
Zhao, Q., Sheng, T., Wang, Y., Tang, Z., Chen, Y., Cai, L. and Ling, H. (2019), "M2Det: A single-shot object detector based on multi-level feature pyramid network", *Proceedings of the AAAI Conference on Artificial Intelligence*, **33**(1), 9259-9266. https://doi.org/10.1609/aaai.v33i01.33019259.
Zhao, C., Liu, X., Zhong, S., Shi, K., Liao, D. and Zhong, Q. (2021a), "Secure consensus of multi-agent systems with redundant signal and communication interference via distributed dynamic event-triggered control", *ISA T.*, **112**, 89-98. https://doi.org/10.1016/j.isatra.2020.11.030.
Zhao, Y., Moradi, Z., Davoudi, M. and Zhuang, J. (2021b), "Bending and stress responses of the hybrid axisymmetric system via state-space method and 3D-elasticity theory", *Eng. Comput.*, 1-23. https://doi.org/10.1007/s00366-020-01242-1.
Zheng, W., Xun, Y., Wu, X., Deng, Z., Chen, X. and Sui, Y. (2021), "A comparative study of class rebalancing methods for security bug report classification", *IEEE T. Reliab.*, **70**(4), 1658-1670. https://doi.org/10.1109/TR.2021.3118026.
Zhong, L., Fang, Z., Liu, F., Yuan, B., Zhang, G. and Lu, J. (2021), "Bridging the theoretical bound and deep algorithms for open set domain adaptation", *IEEE T. Neural Network.*, 1-15. https://doi.org/10.1109/TNNLS.2021.3119965.
Zhou, W., Yu, L., Zhou, Y., Qiu, W., Wu, M.W. and Luo, T. (2018), "Local and global feature learning for blind quality evaluation of screen content and natural scene images", *IEEE T. Image Process.*, **27**(5), 2086-2095. https://doi.org/10.1109/TIP.2018.2794207.
Zhou, C., Zhao, Y., Zhang, J., Fang, Y. and Habibi, M. (2020a), "Vibrational characteristics of multi-phase nanocomposite reinforced circular/annular system", *Adv. Nano Res.*, **9**(4), 295-307. https://doi.org/10.12989/anr.2020.9.4.295.
Zhou, X.L., Wang, E.G., Lin, Q., Dong, G.P., Wu, W., Huang, K., Lai, C., Yu, G., Zhou, H.C., Ma, X.H., Jia, X., Shi, L., Zheng, Y.S., Liu, L.X., Ha, D., Ni, H., Yang, J. and Fu, J.F. (2020b), "Diagnostic performance of convolutional neural network-based Tanner-Whitehouse 3 bone age assessment system", *Quant Imag. Med. Surg.*, **10**(3), 657-667. https://doi.org/10.21037/qims.2020.02.20.